Chapter 5

Potent Blue Emitting Ambipolar Fluorenes Dopants for Enhancing the Performance of Deep Blue Organic Light-Emitting Devices

5-1 Introduction

High efficient red, green, and blue light-emitting devices are basic elements for high resolution full color organic light-emitting devices.[1] High efficient red and green OLEDs have already been described, but high brightness, stable, and efficient blue light-emitting devices with satisfied color purity (CIE coordinate, x = ~0.15, y = ~0.15) still great challenge to develop.[2] From chemical properties of view, it is rather difficult to distinguish between carriers transporting and emitting materials. Generally, emitting materials possess bipolar carrier transport properties but having either major electron transport characteristics or major hole transport characteristics. A number of blue light-emitting materials have been explored, most of these materials owning a high energy band gaps (~3.0 eV), for example of blue emitting materials based on distyrylarylenes,[3] diarylanthrances,[4] spirobifluorenes,[5] oligofluorenes,[6] quinoline,[7] oxadiazole[8] and siloles[9] have been developed. These blue florophores have either low LUMO's (The Lowest Unoccupied Molecular Orbital) levels or high HOMO's (The Highest Occupied Molecular Orbital) levels. Low LUMO's level (EA ≤ 2.5 eV) of or high HOMO's level (IP ≥ 5.9 eV) would make it difficult to inject electron or hole leading to poor device EL performance.

Recently, triarylamino pendent stilbene fluorphores, promising blue emitting materials, have been developed for a series of doped blue OLEDs.[2a, 3c, 10, 11] Such hole transportable emitting materials need to doped into a wide bandgap host, for example of 4,4'-bis-(2,2-diphenyl-vinyl)-biphenyl (**DPVBi**),[11] 9,10-di-naphthalen-2-yl-anthracene (**AND**),[4a] or 2-methyl-9,10-di-naphthalen-2-yl-anthracene (**MADN**) [2a, 3c, 10] (**Figure 5-1**). The significant enhancement of blue OLEDs efficiencies were due to the improvement of electron

injection and transport.

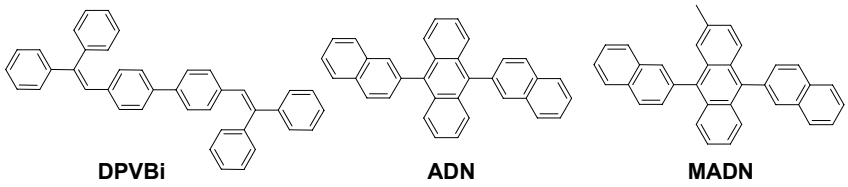

Figure 5-1. The chemical structures of **DPVBi**, **AND**, and **MADN**.

In 1995, **DPVBi** was reported as an efficient host material by Hosokawa and coworkers at Idemitsu company (**Figure 5-2**), that applied to OLED of ITO/CuPc/TPD/**DPVBi**:**BCzVBi**/Alq_3/Mg:Ag displays external quantum efficiency of 2.4%.[11] Although there is efficient energy transfer from **DPVBi** to **BCzVBi**, such OLED showed EL emission of unsatisfactory sky blue color. Chen et al. doped the blue emitting material **DSA-Ph** (**Figure 5-2**) into **MADN** is the device of ITO/CFx/NPB:CuPc/NPB/ **MADN**:**DSA-Ph**/Alq_3/LiF/Al. [2a] The device achieved a high EL efficiency of 9.7 cd/A with a greenish-blue emission of CIE coordinate, x = 0.16, y = 0.32. In order to improve the unsatisfactory greenish-blue color, **BD-1** (**Figure 5-2**) was further developed as a deep blue emitting material for the device of ITO/CFx/NPB:CuPc/NPB/**MADN**:**BD-1**/Alq_3/LiF/Al. The optimal **BD-1** concentration of 5% showed a satisfactory deep blue (CIE coordinate x = 0.14, y = 0.13) EL with current efficiency of 5.4 cd/A or external quantum efficiency of 5.1% at current density of 20 mA/cm^2. [10c] It also exhibits high electroluminescence of 1080 cd/m^2 at current density of 20 mA/cm^2. To the best of our knowledge, this is one of the best blue OLEDs reported in literature. Before **MADN,** its analog **ADN** was reported as a host for **TBP** dopant by Shi and Tang at Kodak company (**Figure 5-2**).[4a] Liu *et al.*[12] recently reported a series of fluoro substituted diphenyl-aminoarylenevinylene 5a (**Figure 5-2**), which has a similar structure to that of **DSA-Ph**. The fluorescence of such compound was tuned to authentic blue color. It takes electron withdrawing fluoro substituent to abate the strength of diaryamino donor group resulting a decrease of HOMO energy level and hence a wider

energy gap. **ADN** was selected as the host material for fluoro dopant **5a** in OLED of ITO/ CuPc/NPB/**ADN**:**5a**/Alq_3/Mg:Ag. It showed a remarkable external quantum efficiency of 4.8% at the current density of 20 mA/cm^2, and the maximum brightness at 10 V is 22506 cd/m^2 with CIE coordinate, x = 0.14, y = 0.14.

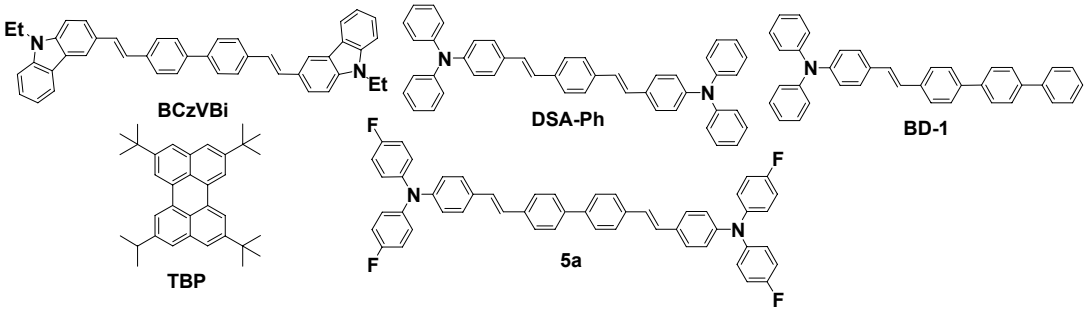

Figure 5-2. The chemical structures of **BCzVBi**, **DSA-Ph**, **BD-1**, **TBP**, and **5a**.

5-2 Motivation of research

In 2006, Okumoto reported an efficient electron transporting material of 9,10-bis(4-(6-methylbenzothiazol-2-yl)phenyl)anthracene (**DBzA**) (**Figure 5-3**) used in the red OLED ITO/CFx/NPB/Rubrene:**DBP** (1%)/**DBzA**/LiF/Al.[13] Such OLED showed current efficiency of 5.4 cd/A, which is a 2.5 times high their Alq_3-based device ITO/CFx/NPB/ Rubrene:**DBP** (1%)/Alq_3/LiF/Al (current efficiency = 2.1 cd/A). This is mainly due to the electron transporting feature of benzothiazole moiety of **DBzA**. In Chapter 2, 3 and 4, the diphenylamine-containg fluorene or spiro- bifluorene was demonstrated as very good materials for OLED, mainly due to their high solid state fluorescent quantum yield and high thermal morphological stability. In addition to the hole transporting characteristic of triarylamine moiety, we introduced electron transporting benzothiazole moiety in order to balance the hole and electron carriers in OLEDs. In addition, changing the substituent of diphenylamino group, fluorescence of these fluorophores can be easily tuned to the desired deep blue color (**Figure 5-4**).

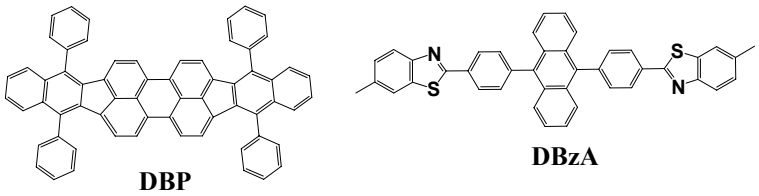

Figure 5-3. The chemical structures of DBP and **DBzA**.

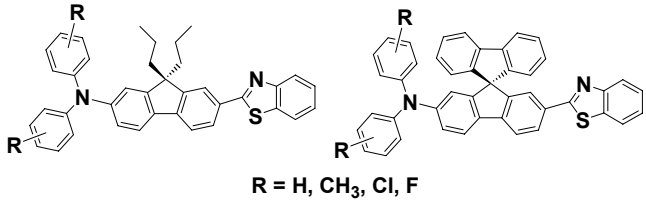

Figure 5-4. Ambipolar design of fluorene- and spirobifluorene-based blue fluorophores.

5-3 Experimental

5-3-1 Materials

The synthesis of 7-bromo-9,9-dipropylfluorene-2-carboxaldehyde and 7-bromo-9,9-spirobifluorene-2-carboxaldehyde were descried in chapter 2. Di-*o*-tolylamine, bis(2-fluoro-phenyl)amine, bis(2-chloro-phenyl)amine, and bis(2,4-difluorophenyl)amine were synthesized according to literature procedures. 2-Aminobenzenethiol, DMSO, *n*-butyllithium (*n*-BuLi) 1.6 M in hexane, iodine, di- phenylamine, palladium(II) acetate ($Pd(OAc)_2$) with 47.5% palladium, tri-*tert*-butylphosphine 99% ($P(^tBu)_3$), cesium carbonate (Cs_2CO_3), malononitrile, basic aluminum oxide (Al_2O_3), *N*,*N*'-dimethylformamide (DMF), tetrahydrofuran (THF), calcium hydride, benzophenone, toluene, dichloromethane, ethyl acetate, and hexane were purchased from Acros, Fluka, Aldrich, Riedel-dehaën, TCI, Merck or Mallunckrodt. DMF was distilled by calcium sulfate under reduced pressure. Toluene was distilled under nitrogen from calcium hydride. THF was distilled under nitrogen from sodium benzophenone ketyl, and other solvents were dried using standard procedures. All commercial reagents were used as received unless otherwise stated.

5-3-2 Instrument

All of the measurement methods of instruments were similar to the description of 2-3-1 in Chapter 2

5-3-3 Synthesis

Synthesis of 2-(7-bromo-9,9'-dipropyl-9*H*-fluoren-2-yl)benzothiazole (BrFBT)

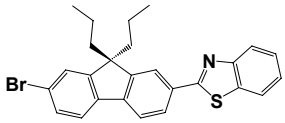

BrFBT

Under nitrogen atmosphere, a mixture of 7-bromo-9,9-dipropylfluorene-2-carboxaldehyde (10 g, 28 mmol) and 2-aminobenzenethiol (4.2 g, 33.6 mmol) are stirred in DMSO (50 mL) for 6 h at 180 ^{o}C. After cooling to room temperature, the precipitate was filtrated and washed with water. The residue was subjected to flash column chromatography (silica gel, dichloromethane/hexanes: 1/5). A white solid was obtained. Yield: 93% (12 g). ^{1}H NMR (400 MHz, $CDCl_3$): δ (ppm) 8.11 (d, 1H, *J* = 1.6 Hz), 8.08 (d, 1H, *J* = 7.8 Hz), 8.01 (dd, 1H, *J* = 7.9 Hz, 1.6 Hz), 7.90 (d, 1H, *J* = 8.0 Hz), 7.73 (d, 1H, *J* = 7.9 Hz), 7.59 (d, 1H, *J* = 8.0 Hz), 7.40–7.60 (m, 3H), 7.38 (t, 1H, *J* = 7.9 Hz), 1.90–2.10 (m, 4H), 0.60–0.70 (m, 10H). ^{13}C NMR (100 MHz, $CDCl_3$): δ (ppm) 168.4, 154.2, 153.6, 151.2, 142.9, 139.1, 134.9, 132.7, 130.2, 127.2, 126.34, 126.31, 125.1, 123.0, 122.1, 121.6, 121.5, 120.2, 55.9, 42.5, 17.1, 14.3. FAB-MS: calcd. MW, 461.1, m/e = 462.0 $(M+H)^{+}$.

Synthesis of 2-(7-bromo-9,9'-spirobifluoren-2-yl)-benzothiazole (BrSPBT)

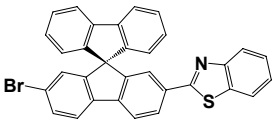

BrSPBT

Under nitrogen atmosphere, a mixture of 7-bromo-9,9-spirobifluorene-2-carboxaldehyde (6 g, 14.2 mmol) and 2-aminobenzenethiol (1.9 g, 15 mmol) are stirred in DMSO (20 mL) for 6 h at 180 ^{o}C. After cooling to room temperature, the precipitate was

filtrated and washed with water. The residue was subjected to flash column chromatography (silica gel, dichloromethane/hexanes: 1/5). A white solid was obtained. Yield: 80% (6 g). ^{1}H NMR (400 MHz, $CDCl_3$): δ (ppm) 8.08 (dd, 1H, *J* = 8.0 Hz, 1.7 Hz), 7.93 (dd, 1H, *J* = 8.0 Hz), 7.90 (d, 1H, *J* = 7.9 Hz), 7.87 (d, 2H, *J* = 7.6 Hz), 7.79 (d, 1H, *J* = 8.0 Hz), 7.73 (d, 1H, *J* = 8.1 Hz), 7.50 (dd, 1H, *J* = 8.2 Hz, 1.8 Hz), 7.49 (s, 1 H), 7.50 (t, 1H, *J* = 8.0 Hz), 7.50 (t, 2H, *J* = 7.6 Hz), 7.31 (t, 1H, *J* = 8.1 Hz), 7.12 (t, 1H, *J* = 7.6 Hz), 6.84 (d, 1H, *J* = 1.7 Hz), 6.74 (d, 2H, *J* = 7.6 Hz). ^{13}C NMR (100 MHz, $CDCl_3$): δ (ppm) 167.7, 153.9, 151.7, 149.4, 147.1, 143.6, 141.9, 139.5, 134.8, 133.5, 131.1, 128.2, 128.09, 128.07, 127.3, 126.3, 125.1, 124.1, 123.0, 122.9, 122.5, 121.8, 121.5, 120.5, 120.3, 65.8. EI-MS: calcd. MW, 527.03, m/e = 528.05/530.05 $(M+H)^+$.

Synthesis of 2-(7-iodo-9,9'-dipropyl-9*H*-fluoren-2-yl)benzothiazole (IFBT)

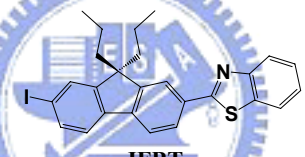

IFBT

To a THF solution (20 mL) containing **BrFBT** (1 g, 2.17 mmol), *n*-BuLi (1.5 mL, 2.4 mmol, 1.6 M in hexane) was added slowly at −78 °C. The mixture was stirred for 2 h under nitrogen atmosphere. After the slow addition of I_2 (0.61 g, 2.4 mmol) THF (5 mL) solution, the reaction solution was kept at −78 °C for 1 h. The reaction mixture was then warmed to room temperature and stirred overnight. After drying by sodium sulfite, the solution was extracted with ethyl acetate, dried over $MgSO_4$, and concentrated under reduced pressure. The residue was subjected to flash column chromatography (silica gel, dichloromethane/hexanes: 1/10) to give white solid. Yield: 86% (0.95 g). ^{1}H NMR (400 MHz, $CDCl_3$): δ (ppm) 8.10 (d, 1H, *J* = 1.5 Hz), 8.08 (d, 1H, *J* = 8.1 Hz), 8.01 (dd, 1H, *J* = 7.9 Hz, 1.6 Hz), 7.90 (d, 1H, *J* = 8.0 Hz), 7.74 (d, 1H, *J* = 7.9 Hz), 7.70 (d, 1H, *J* = 1.4 Hz), 7.67 (dd, 1H, *J* = 7.9 Hz, 1.5 Hz), 7.49 (t, 1H, *J* = 8.1 Hz), 7.47 (d, 1H, *J* = 7.9 Hz), 7.38 (t, 1H, *J* = 8.0 Hz), 1.85-2.10 (m, 4H), 0.61-0.70 (m, 10H). ^{13}C NMR (100 MHz, $CDCl_3$): δ (ppm)

168.4, 154.2, 153.8, 151.0, 143.0, 139.7, 136.1, 134.9, 132.9, 132.2, 127.2, 126.3, 125.1, 123.0, 121.9, 121.5, 121.45, 120.2, 93.7, 55.8, 42.4, 17.1, 14.3. FAB-MS: calcd. MW, 509.07, m/e = 510.1 $(M+H)^+$.

Synthesis of 2-(7-iodo-9,9'-spirobifluoren-2-yl) benzothiazole (ISPBT)

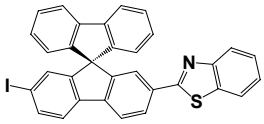

ISPBT

To a THF solution (30 mL) containing **BrSPBT** (1.5 g, 2.85 mmol), *n*-BuLi (1.9 mL, 3.14 mmol, 1.6 M in hexane) was added slowly at −78 °C. The mixture was stirred for 2 h under nitrogen atmosphere. After the slow addition of I_2 (0.8 g, 3.14 mmol) THF (10 mL) solution, the reaction solution was kept at −78 °C for 1 h. The reaction mixture was then warmed to room temperature and stirred overnight. After drying by sodium sulfite, the solution was extracted with ethyl acetate, dried over $MgSO_4$, and concentrated under reduced pressure. The residue was subjected to flash column chromatography (silica gel, dichloromethane/hexanes: 1/5) to give white solid. Yield: 73% (1.2 g). ^{1}H NMR (400 MHz, $CDCl_3$): δ (ppm) 8.07 (dd, 1H, *J* = 8.0 Hz, 1.6 Hz), 7.92 (d, 1H, *J* = 7.7 Hz), 7.90 (d, 1H, *J* = 8.0 Hz), 7.87 (d, 2H, *J* = 7.6 Hz), 7.79 (d, 1H, *J* = 7.9 Hz), 7.71 (dd, 1H, *J* = 8.0 Hz, 1.5 Hz), 7.61 (d, 1H, *J* = 8.0 Hz), 7.49 (d, 1H, *J* = 1.5 Hz), 7.40 (t, 1H, *J* = 8.0 Hz), 7.39 (t, 2H, *J* = 7.6 Hz), 7.30 (t, 1H, *J* = 8.0 Hz), 7.12 (d, 2H, *J* = 7.6 Hz), 7.03 (d, 1H, *J* = 1.4 Hz), 6.74 (d, 2H, *J* = 7.6 Hz). ^{13}C NMR (100 MHz, $CDCl_3$): δ (ppm) 167.7, 153.9, 151.8, 149.2, 147.1, 143.6, 141.9, 140.2, 137.0, 134.8, 133.6, 133.1, 128.2, 128.1, 126.3, 125.1, 124.9, 122.9, 121.5, 120.5, 120.3, 94.1, 65.7. EI-MS: calcd. MW, 575.02, m/e = 576.03 $(M+H)^+$.

Synthesis of (7-benzothiazol-2-yl-9,9'-dipropyl-9*H*-fluoren-2-yl) diphenylamine (PhFBT)

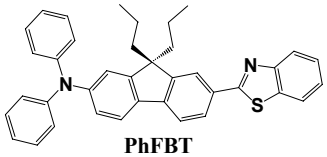

PhFBT

Under nitrogen atmosphere, a mixture of **BrFBT** (1 g, 2.16 mmol), di-phenylamine (0.44 g, 2.6 mmol), $Pd(OAc)_2$ (0.013 g, 0.06 mmol, 2.5 mol%), $P(^tBu)_3$ (0.024 g, 0.12 mmol, 5 mol%), and Cs_2CO_3 (1 g, 3.1 mmol) in toluene (10 mL) was heated at 120 ^oC with stirring for 12 h. After cooling to room temperature, saturated ammonium chloride solution was added to the reaction solution. The solution was extracted with ethyl acetate and dried over $MgSO_4$. After the removal of $MgSO_4$, the solution was concentrated under reduced pressure and subjected to flash column chromatography (silica gel, dichloromethane/hexanes: 1/2). A greenish yellow solid was obtained. Yield: 92% (1.1 g). ^1H NMR (400 MHz, $CDCl_3$): δ (ppm) 8.07 (s, 1H), 8.06 (d, 1H, J = 7.5 Hz), 7.98 (dd, 1H, J = 7.9 Hz, 1.6 Hz), 7.89 (d, 1H, J = 7.5 Hz), 7.66 (d, 1H, J = 7.9 Hz), 7.57 (d, 1H, J = 8.2 Hz), 7.47 (t, 1H, J = 7.5 Hz), 7.36 (t, 1H, J = 7.5 Hz), 7.20–7.24 (m, 4H), 7.09–7.15 (m, 4H), 6.95–7.10 (m, 3H), 1.80–2.02 (m, 4H), 0.60-0.74 (m, 10H). ^{13}C NMR (100 MHz, $CDCl_3$): δ (ppm) 169.1, 154.2, 152.9, 151.4, 148.1, 147.8, 144.1, 134.9, 134.8, 131.4, 129.2, 127.2, 126.2, 124.9, 124.1, 123.0, 122.9, 122.8, 121.5, 121.4, 120.9, 119.3, 118.7, 55.5, 42.4, 17.3, 14.4. EI-MS: calcd. MW, 550.24, m/e = 551.17 $(M+H)^+$. Anal. Found (calcd.) for $C_{38}H_{34}N_2S$: C 82.74 (82.87), H 6.35 (6.22), N 5.04 (5.09)

Synthesis of (7-benzothiazol-2-yl-9,9'-spirobifluoren-2-yl)diphenylamine (PhSPBT)

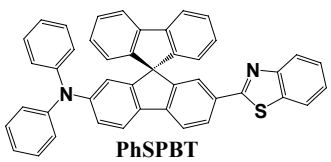

PhSPBT

Under nitrogen atmosphere, a mixture of **BrSPBT** (0.7 g, 1.3 mmol), di- phenylamine

(0.63 g, 1.56 mmol), $Pd(OAc)_2$ (0.007 g, 0.03 mmol, 2.5 mol%), $P(^tBu)_3$ (0.012 g, 0.06 mmol, 5 mol%), and Cs_2CO_3 (0.6 g, 1.8 mmol) in toluene (5 mL) was heated at 120 °C with stirring for 12 h. After cooling to room temperature, saturated ammonium chloride solution was added to the reaction solution. The solution was extracted with ethyl acetate, dried over $MgSO_4$. After the removal $MgSO_4$, the he solution was concentrated under reduced pressure and subjected to flash column chromatography (silica gel, dichloromethane/hexanes: 1/2). A greenish yellow solid was obtained. Yield: 92% (0.74 g). ^1H NMR (400 MHz, $CDCl_3$): δ (ppm) 8.03 (dd, 1H, *J* = 8.0 Hz, 1.7 Hz), 7.89 (d, 1H, *J* = 8.0 Hz), 7.80 (d, 1H, *J* = 8.0 Hz), 7.78 (d, 1H, *J* = 8.0 Hz), 7.75 (d, 2H, *J* = 7.6 Hz), 7.69 (d, 1H, *J* = 8.3 Hz), 7.42 (d, 1H, *J* = 1.6 Hz), 7.39 (t, 1H, *J* = 8.0 Hz), 7.33 (d, 2H, *J* = 7.5 Hz), 7.28 (t, 1H, *J* = 8.0 Hz), 7.05–7.15 (m, 6H), 6.99 (dd, 1H, *J* = 8.3 Hz, 2.1 Hz), 6.80–6.95 (m, 6H), 6.82 (d, 2H, *J* = 7.6 Hz), 6.51 (d, 1H, *J* = 2.1 Hz). ^{13}C NMR (100 MHz, $CDCl_3$): δ (ppm) 168.2, 154.0, 151.2, 149.5, 148.4, 148.0, 147.3, 144.6, 141.8, 135.1, 134.8, 132.1, 129.1, 128.0, 127.83, 127.79, 126.2, 124.9, 124.1, 123.9, 123.6, 122.9, 122.79, 122.78, 121.4, 121.2, 120.2, 119.7, 119.1, 65.9. EI-MS: calcd. MW, 616.20, m/e = 617.21 $(M+H)^+$. Anal. Found (calcd.) for $C_{44}H_{28}N_2S$: C 85.34 (85.68), H 4.52 (4.58), N 4.40 (4.54)

Synthesis of (7-benzothiazol-2-yl-9,9'-dipropyl-9*H*-fluoren-2-yl)di-*o*-tolylamine (oTFBT)

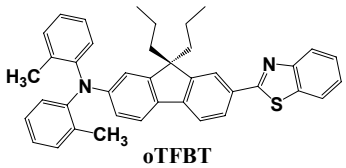

oTFBT

A mixture of **IFBT** (1.2 g, 1.96 mmol), di-*o*-tolylamine (0.59 g, 3.0 mmol), K_2CO_3 (1.08 g, 7.8 mmol), Cu (0.25 g, 3.92 mmol), and 18-crown-6 (0.04 g, 0.15 mmol) was stirred in 1,2-dichlorobenzene (10 mL) at 200 °C for 48 h. After cooling to room temperature, the reaction solution was filtered. The filtrate was subjected to flash column chromatography

(silica gel, dichloromethane/hexanes: 1/2). A greenish yellow solid was obtained. Yield: 83% (0.95 g). ^{1}H NMR (400 MHz, $CDCl_3$): δ (ppm) 8.05 (d, 1H, *J* = 7.9 Hz), 8.03 (d, 1H, *J* = 1.7 Hz), 7.95 (dd, 1H, *J* = 7.9 Hz, 1.6 Hz), 7.88 (d, 1H, *J* = 7.9 Hz), 7.61 (d, 1H, *J* = 8.1 Hz), 7.49 (d, 1H, *J* = 7.4 Hz), 7.47 (t, 1H, *J* = 7.9 Hz), 7.35 (t, 1H, *J* = 7.9 Hz), 7.21 (d, 2H, *J* = 7.2 Hz), 7.06–7.16 (m, 4H), 6.99 (d, 2H, *J* = 7.6 Hz), 6.65 (dd, 1H, *J* = 7.4 Hz, 2.1 Hz), 6.64 (s, 1H), 2.02 (s, 6H), 1.74-1.79 (m, 4H), 0.63–0.68 (m, 10H). ^{13}C NMR (100 MHz, $CDCl_3$): δ (ppm) 169.0, 154.2, 153.0, 151.0, 149.2, 146.0, 144.5, 134.9, 134.5, 132.7, 131.7, 130.9, 127.4, 127.1, 127.0, 126.20, 124.84, 124.80, 122.8, 121.5, 121.3, 120.8, 119.3, 118.9, 114.2, 55.4, 42.5, 18.9, 17.2, 14.4. EI-MS: calcd. MW, 578.28, m/e = 579.19 $(M+H)^+$. Anal. Found (calcd.) for $C_{40}H_{38}N_2S$: C 82.94 (83.00), H 6.45 (6.62), N 4.70 (4.84)

Synthesis of (7-benzothiazol-2-yl-9,9'-spirobifluoren-2-yl)di-*o*-tolylamine (oTSPBT)

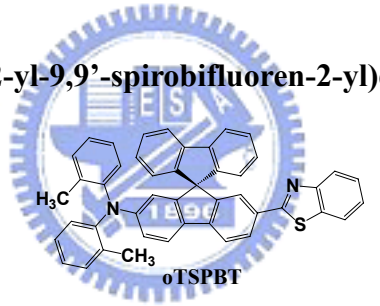

oTSPBT

A mixture of **ISPBT** (1.2 g, 2.1 mmol), di-*o*-tolylamine (0.62 g, 3.1 mmol), K_2CO_3 (1.16 g, 8.4 mmol), Cu (0.27 g, 4.2 mmol), and 18-crown-6 (0.056 g, 0.21 mmol) was stirred in 1,2-dichlorobenzene (10 mL) at 200 ^{o}C for 48 h. After cooling to room temperature, the reaction solution was filtered. The filtrate was subjected to flash column chromatography (silica gel, dichloromethane/hexanes: 1/2). A greenish yellow solid was obtained. Yield: 67% (0.9 g). ^{1}H NMR (400 MHz, $CDCl_3$): δ (ppm) 8.01 (dd, 1H, *J* = 8.0 Hz, 1.7 Hz), 7.89 (d, 1H, *J* = 8.1 Hz), 7.73–7.78 (m, 4H), 7.63 (d, 1H, *J* = 8.4 Hz), 7.25–7.40 (m, 6H), 7.09 (t, 2H, *J* = 7.5 Hz), 6.85–7.10 (m, 8H), 6.79 (d, 2H, *J* = 7.6 Hz), 6.65 (dd, 1H, *J* = 8.4 Hz, 2.2 Hz), 5.98 (d, 1H, *J* = 2.2 Hz). ^{13}C NMR (100 MHz, $CDCl_3$): δ (ppm) 168.3, 154.0, 151.0, 149.4, 149.2, 148.2, 145.0, 141.8, 134.8, 132.9, 131.5, 127.9, 127.7, 126.8, 126.1, 124.8,

123.9, 122.7, 122.6, 121.4, 121.0, 120.2, 119.7, 119.2, 114.6, 65.9, 18.8. EI-MS: calcd. MW, 644.23, m/e = 645.23 $(M+H)^+$. Anal. Found (calcd.) for $C_{46}H_{32}N_2S$: C 85.22 (85.68), H 4.87 (5.00), N 4.19 (4.34)

Synthesis of (7-benzothiazol-2-yl-9,9'-dipropyl-9*H*-fluoren-2-yl)bis(2-chlorophenyl) amine (oClPhFBT)

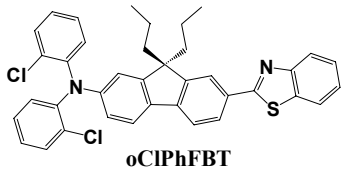

oClPhFBT

A mixture of **IFBT** (1.2 g, 1.96 mmol), bis(2-chloro-phenyl)amine (0.71 g, 3.0 mmol), K_2CO_3 (1.08 g, 7.8 mmol), Cu (0.25 g, 3.92 mmol), and 18-crown-6 (0.04 g, 0.15 mmol) was stirred in 1,2-dichlorobenzene (10 mL) at 200 °C for 48 h. After cooling to room temperature, the reaction solution was filtered. The filtrate was subjected to flash column chromatography (silica gel, dichloromethane/hexanes: 1/2). A canary yellow solid was obtained. Yield: 71% (0.85 g). ^{1}H NMR (400 MHz, $CDCl_3$): δ (ppm) 8.06 (d, 1H, *J* = 7.9 Hz), 8.05 (s, 1H), 7.96 (dd, 1H, *J* = 7.9 Hz, 1.5 Hz), 7.88 (d, 1H, *J* = 7.9 Hz), 7.64 (d, 1H, *J* = 7.9 Hz), 7.54 (d, 1H, *J* = 7.5 Hz), 7.46 (t, 1H, *J* = 8.0 Hz), 7.43 (d, 2H, *J* = 8.0 Hz), 7.35 (t, 1H, *J* = 8.0 Hz), 7.22 (d, 2H, *J* = 8.1 Hz), 7.11-7.17 (m, 4H), 6.69 (s, 1H), 6.67 (dd, 1H, *J* = 7.5 Hz, 2.1 Hz), 1.75–2.01 (m, 4H), 0.64-0.71 (m, 10H). ^{13}C NMR (100 MHz, $CDCl_3$): δ (ppm) 169.0, 154.2, 152.9, 151.3, 147.6, 144.3, 143.8, 134.9, 133.9, 131.5, 131.3, 131.2, 129.0, 127.7, 127.2, 126.2, 124.9, 122.9, 121.5, 121.3, 120.7, 119.4, 119.2, 114.7, 55.5, 42.6, 17.1, 14.4. EI-MS: calcd. MW, 618.08, m/e = 619.09/621.08/623.08 $(M+H)^+$. Anal. Found (calcd.) for $C_{38}H_{32}Cl_2N_2S$: C 73.35 (73.66), H 5.13 (5.21), N 4.41 (4.52)

Synthesis of (7-benzothiazol-2-yl-9,9'-spirobifluoren-2-yl)bis(2-chlorophenyl)amine (oClPhSPBT)

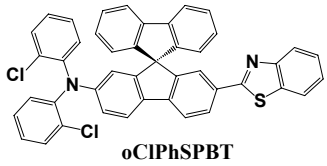

oClPhSPBT

A mixture of **ISPBT** (1.5 g, 2.61 mmol), bis(2-chloro-phenyl)amine (0.93 g, 3.92 mmol), K_2CO_3 (1.44 g, 10.4 mmol), Cu (0.33 g, 5.2 mmol), and 18-crown-6 (0.07 g, 0.26 mmol) was stirred in 1,2-dichlorobenzene (10 mL) at 200 ^oC for 48 h. After cooling to room temperature, the reaction solution was filtered. The filtrate was subjected to flash column chromatography (silica gel, dichloromethane/hexanes: 1/2). A canary yellow solid was obtained. Yield: 62% (1.1 g). ^1H NMR (400 MHz, $CDCl_3$): δ (ppm) 8.00 (dd, 1H, J = 8.0 Hz, 1.6 Hz), 7.89 (d, 1H, J = 8.0 Hz), 7.74–7.80 (m, 4H), 7.68 (d, 1H, J = 8.3 Hz), 7.24–7.40 (m, 7H), 7.10 (t, 2H, J = 7.6 Hz), 7.06 (d, 2H, J = 7.6 Hz), 6.96-7.03 (m, 4H), 6.79 (d, 1H, J = 7.6 Hz), 6.69 (dd, 1H, J = 8.3 Hz, 2.2 Hz), 6.07 (d, 1H, J = 2.2 Hz). ^{13}C NMR (100 MHz, $CDCl_3$): δ (ppm) 168.2, 154.0, 150.9, 149.6, 148.0, 147.8, 144.7, 143.3, 141.7, 134.8, 134.3, 131.9, 131.3, 131.1, 128.8, 127.9, 127.8, 127.7, 127.6, 126.1, 124.9, 124.1, 122.7, 122.65, 121.4, 120.9, 120.0, 119.5, 115.7, 65.9. EI-MS: calcd. MW, 684.12, m/e = 685.13/687.13 $(M+H)^+$. Anal. Found (calcd.) for $C_{44}H_{26}Cl_2N_2S$: C 76.84 (77.07), H 3.63 (3.82), N 3.86 (3.86)

Synthesis of (7-benzothiazol-2-yl-9,9'-dipropyl-9*H*-fluoren-2-yl)bis(2-fluorophenyl) amine (oFPhFBT)

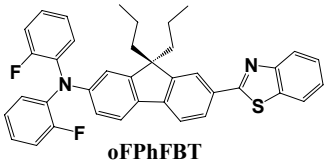

oFPhFBT

Under nitrogen atmosphere, a mixture of **BrFBT** (2 g, 4.34 mmol), bis(2-fluoro-

phenyl)amine (1.16 g, 5.64 mmol), $Pd(OAc)_2$ (0.025 g, 0.11 mmol, 2.5 mol%), $P(^tBu)_3$ (0.044 g, 0.22 mmol, 5 mol%), and Cs_2CO_3 (2 g, 6.21 mmol) in toluene (15 mL) was heated at 120 ^oC with stirring for 12 h. After cooling to room temperature, saturated ammonium chloride solution was added to the reaction solution. The solution was extracted with ethyl acetate, and dried over $MgSO_4$. After the removal of $MgSO_4$, the solution was concentrated under reduced pressure and subjected to flash column chromatography (silica gel, dichloromethane/hexanes: 1/2). A greenish yellow solid was obtained. Yield: 86% (2.2 g). ^1H NMR (400 MHz, $CDCl_3$): δ (ppm) 8.06 (d, 1H, J = 7.9 Hz), 8.06 (d, 1H, J = 1.4 Hz), 7.96 (dd, 1H, J = 7.9 Hz, 1.6 Hz), 7.88 (d, 1H, J = 7.9 Hz), 7.64 (d, 1H, J = 8.2 Hz), 7.55 (d, 1H, J = 7.9 Hz), 7.47 (t, 1H, J = 7.7 Hz), 7.35 (t, 1H, J = 7.7 Hz), 7.06–7.23 (m, 8H), 6.86 (d, 1H, J = 2.0 Hz), 6.82 (dd, 1H, J = 8.2 Hz, 2.0 Hz), 1.76-2.02 (m, 4H), 0.63–0.72 (m, 10H). ^{13}C NMR (100 MHz, $CDCl_3$): δ (ppm) 168.9, 157.6 (d, J_{CF} = 249.9 Hz), 154.3, 152.9, 151.3, 147.6, 144.3, 134.9, 134.2, 134.1, 131.2, 127.9, 127.2, 126.2, 125.9 (d, J_{CF} = 7.4 Hz), 124.9, 124.7, 122.9. 121.5, 121.4, 120.7, 119.2, 118.7, 116.9 (d, J_{CF} = 19.6 Hz), 114.3, 55.5, 42.6, 17.1, 14.4. EI-MS: calcd. MW, 586.23, m/e = 587.14/588.14 $(M+H)^+$. Anal. Found (calcd.) for $C_{38}H_{32}F_2N_2S$: C 77.59 (77.79), H 5.46 (5.50), N 4.66 (4.77)

Synthesis of (7-benzothiazol-2-yl-9,9'-spirobifluoren-2-yl)bis(2-fluorophenyl)amine (oFPhSPBT)

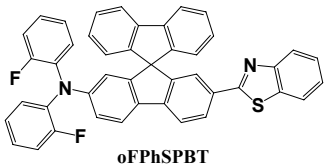

oFPhSPBT

Under nitrogen atmosphere, a mixture of **BrSPBT** (1 g, 1.9 mmol), bis(2-fluoro-phenyl)amine (0.55 g, 2.3 mmol), $Pd(OAc)_2$ (0.011 g, 0.05 mmol, 2.5 mol%), $P(^tBu)_3$ (0.02 g, 0.1 mmol, 5 mol%), and Cs_2CO_3 (0.9 g, 2.76 mmol) in toluene (10 mL) was heated at 120 ^oC

with stirring overnight. After cooling to room temperature, saturated ammonium chloride solution was added to the reaction solution. The solution was extracted with ethyl acetate, dried over $MgSO_4$. After the removal of $MgSO_4$, the solution was concentrated under reduced pressure and subjected to flash column chromatography (silica gel, dichloromethane/hexanes: 1/2). A greenish yellow solid was obtained. Yield: 81% (1.0 g). ^{1}H NMR (400 MHz, $CDCl_3$): δ (ppm) 8.01 (dd, 1H, J = 8.0 Hz, 1.6 Hz), 7.89 (d, 1H, J = 8.1 Hz), 7.70–7.82 (m, 4 H), 7.89 (d, 1H, J = 8.4 Hz), 7.25–7.41 (m, 5 H), 7.11 (t, 2H, J = 7.6 Hz), 6.90–7.05 (m, 4 H), 6.89–6.96 (m, 4 H), 6.78–6.84 (m, 3 H), 6.23 (d, 1H, J = 2.0 Hz). ^{13}C NMR (100 MHz, $CDCl_3$): δ (ppm) 168.2, 158.6156.1, 154.0, 151.0, 149.5, 148.0, 147.9, 144.7, 141.7, 134.8, 134.4, 133.6, 133.5, 131.9, 127.9, 127.8, 127.7, 127.68, 126.1, 126.0, 125.9, 124.9, 124.6, 124.5, 124.0, 122.7, 122.67, 121.4, 120.9, 120.1, 119.5, 119.2, 116.9, 116.7, 114.9, 65.9. EI-MS: calcd. MW, 652.18, m/e =653.19/654.19 $(M+H)^+$. Anal. Found (calcd.) for $C_{44}H_{26}F_2N_2S$: C 80.71 (80.96), H 3.92 (4.01), N 4.22 (4.29)

Synthesis of (7-benzothiazol-2-yl-9,9'-dipropyl-9*H*-fluoren-2-yl)bis(2,4-difluorophenyl) amine (opF2PhFBT)

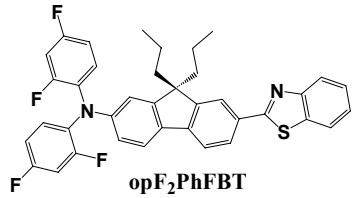

opF$_2$PhFBT

Under nitrogen atmosphere, a mixture of **BrFBT** (2 g, 4.34 mmol)、bis(2,4-difluorophenyl)amine (1.16 g, 5.64 mmol), $Pd(OAc)_2$ (0.025 g, 0.11 mmol, 2.5 mol%), $P(^tBu)_3$ (0.044 g, 0.22 mmol, 5 mol%), and Cs_2CO_3 (2 g, 6.21 mmol) in toluene (15 mL) was heated at 120 ^oC with stirring for 12 h. After cooling to room temperature, saturated ammonium chloride solution was added to the reaction solution. The solution was extracted with ethyl acetate, and dried over $MgSO_4$. After the removal of $MgSO_4$, the solution was

concentrated under reduced pressure and subjected to flash column chromatography (silica gel, dichloromethane/hexanes: 1/2). A greenish yellow solid was obtained. Yield: 89% (2.4 g). ^{1}H NMR (400 MHz, $CDCl_3$): δ (ppm) 8.06 (d, 1H, J = 7.8 Hz), 8.06 (d, 1H, J = 1.3 Hz), 7.96 (dd, 1H, J = 7.9 Hz, 1.6 Hz), 7.88 (d, 1H, J = 7.9 Hz), 7.64 (d, 1H, J = 7.9 Hz), 7.53 (d, 1H, J = 8.2 Hz), 7.47 (t, 1H, J = 8.1 Hz), 7.35 (t, 1H, J = 8.1 Hz), 7.15-7.23 (m, 2 H), 6.83-6.93 (m, 4 H), 6.74 (d, 1H, J = 2.0 Hz), 6.71 (dd, 1H, J = 8.2 Hz, 2.2 Hz), 1.76-2.10 (m, 4H), 0.62-0.72 (m, 10H). ^{13}C NMR (100 MHz, $CDCl_3$): δ (ppm) 168.8, 161.38, 161.35, 158.95, 158.92, 158.88, 156.53, 156.50, 154.2, 153.1, 151.1, 147.5, 144.1, 134.9, 133.8, 131.3, 130.12, 130.08, 130.01, 129.98, 129.03, 128.93, 127.2, 126.2, 124.9, 122.9, 121.5, 121.3, 120.9, 119.2, 117.4, 112.9, 112.03, 112.00, 111.81, 111.78, 105.63, 105.4, 105.14, 112.9, 112.03, 112.00, 111.81, 111.78, 105.63, 105.39, 105.14, 55.5, 42.5, 17.1, 14.4. EI-MS: calcd. MW, 622.21, m/e = 622.0/623.0/624.0/625.0 $(M)^+$. Anal. Found (calcd.) for $C_{38}H_{30}F_4N_2S$: C 73.09 (73.29), H 4.96 (4.86), N 5.02 (4.50)

Synthesis of (7-benzothiazol-2-yl-9,9'-spirobifluoren-2-yl)bis(2,4-difluorophenyl)amine (opF2PhSPBT)

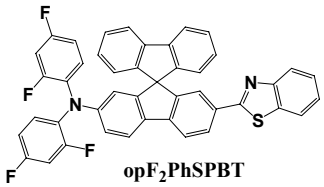

opF$_2$PhSPBT

Under nitrogen atmosphere, a mixture of **BrSPBT** (1 g, 1.9 mmol), bis(2,4-difluorophenyl)amine (0.55 g, 2.3 mmol), $Pd(OAc)_2$ (0.011 g, 0.05 mmol, 2.5 mol%), $P(^tBu)_3$ (0.02 g, 0.1 mmol, 5 mol%), and Cs_2CO_3 (0.9 g, 2.76 mmol) in toluene (10 mL) was heated at 120 ^{o}C with stirring for 12 h. After cooling to room temperature, saturated ammonium chloride solution was added to the reaction solution. The solution was extracted with ethyl acetate, and dried over $MgSO_4$. After the removal of $MgSO_4$, the solution was concentrated under reduced pressure and subjected to flash column chromatography (silica gel,

dichloromethane/hexanes: 1/2). A greenish yellow solid was obtained. Yield: 84% (1.1 g). ^{1}H NMR (400 MHz, $CDCl_3$): δ (ppm) 8.02 (dd, 1H, *J* = 8.0 Hz, 1.6 Hz), 7.89 (d, 1H, *J* = 8.2 Hz), 7.75-8.10 (m, 4H), 7.67 (d, 1H, *J* = 8.4 Hz), 7.40 (d, 1H, *J* = 1.6 Hz), 7.38 (t, 1H, *J* = 7.8 Hz), 7.36 (t, 2H, *J* = 7.5 Hz), 7.30 (t, 1H, *J* = 7.8 Hz), 7.10 (t, 1H, *J* = 7.5 Hz), 6.90-7.12 (m, 2 H), 6.79 (d, 2H, *J* = 7.6 Hz), 6.65–6.75 (m, 5 H), 6.11 (d, 1H, *J* = 2.1 Hz), ^{13}C NMR (125 MHz, $CDCl_3$): δ (ppm) 168.1, 161.3, 161.2, 159.1, 158.88, 158.85, 158.7, 156.5, 156.4, 154.0, 151.3, 149.4, 148.0, 147.8, 144.6, 141.7, 134.8, 134.2, 132.0, 129.64, 129.59, 129.53, 129.49, 128.9, 128.8, 128.0, 127.8, 126.2, 124.9, 124.0, 122.8, 122.7, 121.4, 121.1, 120.1, 119.5, 118.0, 113.7, 111.9, 111.8, 111.7, 111.6, 105.26, 105.24, 105.22, 65.9. EI-MS: calcd. MW, 688.16, m/e = 689.17/690.17/691.17/ 692.17 $(M+H)^{+}$. Anal. Found (calcd.) for $C_{44}H_{24}F_4N_2S$: C 76.32 (76.73), H 3.54 (3.51), N 4.03 (4.07)

5-4 Results and Discussion

5-4-1 Synthesis

Scheme 5-1

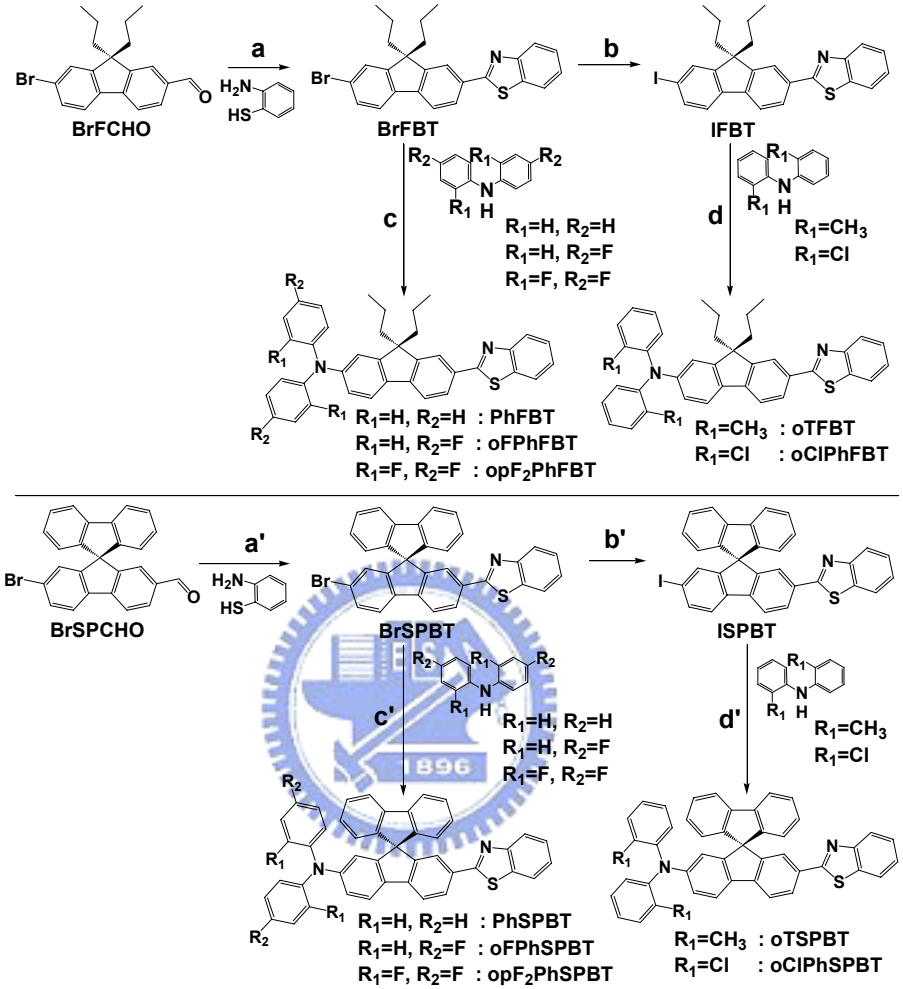

Reagents and conditions: (a and a') DMSO, 200 ^{o}C, 6 h, 93% (**BrFBT**), 80% (**BrSPBT**); (b and b') *n*-BuLi, THF, −78 ^{o}C, then I_2 in THF, RT, overnight, 86% (**IFBT**), 73% (**ISPBT**); (c and c') Cs_2CO_3, $Pd(OAc)_2$, $P(^tBu)_3$, toluene, 120 ^{o}C, overnight, 89% (**PhFBT**), 86% (**oFPhFBT**), 92% (**opF$_2$PhFBT**), 92% (**PhSPBT**), 81% (**oFPhSPBT**), 84% (**opF$_2$PhSPBT**); (d and d') Cu, 18-crown-6 ether, K_2CO_3, 1,2-dichlorobenzene, 180 ^{o}C, 72 h, 67% (**oTFBT**), 62% **(oClPhFBT**), 71% (**oTSPBT**), 83% **(oClPhSPBT**).

The synthetic routes of blue emitting fluorene derivatives are shown in Scheme 5-1. The syntheses are rather similar and straightforward. Either **BrFBT** or **BrSPBT** was obtained by the condensation of **BrFCHO** or **BrSPCHO** and 2- aminobenzenethiol in DMSO with a yield of 93% or 80%, respectively. The following arylamination of the

benzothiazole-carrying fluorene or spirobifluorene derivative, **BrFBT** or **BrSPBT,** was readily performed in the presence of palladium catalyst and a non-nucleophilic base, Cs_2CO_3. Only non-substituted or fluoride substituted at the ortho-position of diphenylamine would take place C-N coupling reaction with **BrFCHO** or **BrSPCHO** under palladium cross coupling condition due to the steric hindrance of ortho chloride or ortho methyl substituted diphenylamine. **PhFBT**, **oFPhFBT**, **opF_2PhFBT**, **PhSPBT**, **oFPhSPBT**, **opF_2PhSPBT** were obtained under palladium cross coupling condition with high yields of 81-92%. Ullmann coupling is another synthetic method of C-N coupling which is a harsh reaction condition with copper catalyst at high temperature. In general, the reactivity of iodide compound would higher than bromide compound. Bromo compound **BrFBT** or **BrSPBT** was easily lithiated with a stoichiometric amount of n-BuLi at −78 ^{o}C, followed by the reaction with iodine to offered **IFBT** or **ISPBT** (86%, or 73%), respectively**.** However, satisfactory reaction yields (62-83%) of ortho chloride or ortho methyl substituted diphenylamino fluorene and spirobifluorene chromophores (**oTFBT**, **oClPhFBT**, **oTSPBT**, **oClPhSPB**) were obtained by the Ullmann coupling reaction of **IFBT** or **ISPBT** and large ortho-substituent-bearing diphenylamines.

5-4-2 Absorption and fluorescence spectroscopic analysis

Normalized optical absorption and fluorescence spectra of benzothiazole-carrying diarylamino fluorene or spirobifluorene derivatives in dilute chlorobenzene solution were showed in **Figure 5-5** and their data are summarized in **Table 5-1**. As expected, the absorption, fluorescence spectra, photoluminescence quantum yield, and energy levels of fluorene derivatives were very similar to spirobifluorene derivative. Those lowest-energy absorption bands of chromophores are thus associated with the charge transfer (CT) transitions from the diaryamino donor to benzothiazole acceptor. In contrast with ortho-unsubstituted chromophores (**PhFBT** or **PhSPBT**), chromophores bearing

ortho-substituent show absorption at 393-374 nm and photoluminescence at 464-439 nm which are comparatively blue-shifted in chlorobenzene. In the cases of **oTFBT** and **oTSPBT**, the ortho-substituent (CH_3) of diphenylamino donor augments the non-planarity of the triarylamine center reducing the extent of π-conjugation between fluorene and diaylamino group and hence the slight blue-shifting of photoluminescence and absorption spectra. By comparing the fluorine or chlorine substituted chromophore **PhFBT** or **PhSPBT**, a large blue-shifting of absorption and fluorescence spectra was observed due to the high electronegativity of fluorine or chlorine substituent which increases the energy band gap by lowering the HOMO energy level of chromophores. High photoluminescence quantum yields (54-74%) of these blue fluorophores were determined by integrating-sphere method (**Table 5-1**). The emission peaks of fluoro- or chloro-substituted fluorophores were shifted to ~450 nm suitable for deep blue OLED application without diminishing fluorescence quantum yield.

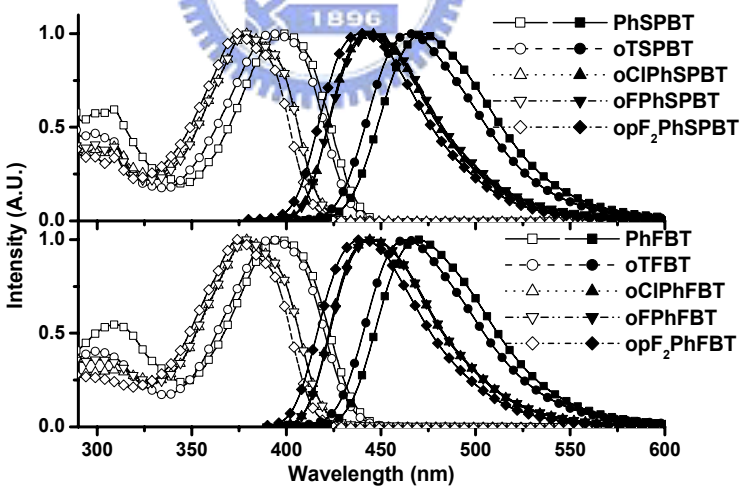

Figure 5-5. Absorption and fluorescence spectra of fluorene and spirobifluorene compounds.

Table 5-1. Optical properties and energy levels of fluorene and spirobifluorene compounds

	In chlorobenzene				HOMO/LUMO (eV/eV)
	λ_{max}^{ab} (nm)	λ_{max}^{fl} (nm)	Φ_f (%)	ΔE (eV, nm)[a]	
PhFBT	396	470	74	2.84, 437	5.58/2.74
oTFBT	393	464	54	2.86, 434	5.63/2.77
oClPhFBT	379	444	61	2.96, 419	5.67/2.71
oFPhFBT	379	446	66	2.96, 419	5.70/2.74
opF$_2$PhFBT	375	440	64	2.99, 415	5.85/2.86
PhSPBT	397	472	72	2.82, 439	5.57/2.75
oTSPBT	393	465	63	2.85, 435	5.63/2.78
oClPhSPBT	379	444	66	2.96, 419	5.76/2.80
oFPhSPBT	379	445	66	2.96, 419	5.77/2.81
opF$_2$PhSPBT	374	439	68	2.99, 414	5.85/2.86

[a]ΔE is the band-gap energy estimated from the low energy edge of absorption spectra.

5-4-3 Electroluminescence properties

5-4-3-1 Devices test of oFPhFBT

Table 5-2. Characteristics of OLEDs containing **oFPhFBT**.

Devices[a]	Max. Luminance (cd/m^2)	Luminance, Efficiency, Voltage at 20 mA/cm^2 (cd/m^2,%, V)[b]	λ_{max}^{el} (nm)	CIE 1931 Chromaticity (x, y)
I	11500	670, 3.8, 8.5	454	0.14, 0.10
II	10900	690, 4.0, 8.6	450	0.14, 0.09
III	3420	360, 2.3, 8.1	454	0.14, 0.09

[a]Device I: ITO/m-TDATA (30 nm)/NPB (20 nm)/**MADN** (40 nm)/Alq_3 (10 nm)/LiF (1 nm)/Al (150 nm); Device II: ITO/m-TDATA (30 nm)/NPB (20 nm)/ **MADN**:**oFPhFBT** (3%, 40 nm)/Alq_3 (10 nm)/LiF (1 nm)/Al (150 nm); Device III: ITO/NPB (30 nm)/CBP (20 nm)/ **TPBI**:**oFPhFBT** (3%, 40 nm)/TPBI (10 nm)/LiF (1 nm)/Al (150 nm); [b]At current density of 20 mA/cm^2.

Firstly, we select **oFPhFBT** for blue dopant in **MADN**-based OLEDs because of its high fluorescence quantum yield (Φ_f = 66%) and desirable emission wavelength (λ_{max}^{fl} = 446 nm). Authentic blue EL was observed for these devices (**Table 5-2** and **Figure 5-6**). The configuration of blue devices was fabricated as Device I: ITO/m-TDATA (30 nm)/NPB (20

nm)/**MADN** (40 nm)/Alq_3 (10 nm)/LiF (1 nm)/Al (150 nm); Device II: ITO/m-TDATA (30 nm)/NPB (20 nm)/ **MADN**:**oFPhFBT** (3%, 40 nm)/Alq_3 (10 nm)/LiF (1 nm)/Al (150 nm); Device III: ITO/NPB (30 nm)/CBP (20 nm)/**TPBI**:**oFPhFBT** (3%, 40 nm)/TPBI (10 nm)/LiF (1 nm)/Al (150 nm). In those devices, m-TDATA, NPB, CBP, Alq_3 and TPBI were used as hole-injecting, hole-transporting, hole-transporting/electronblocking, electron-transporting layers, and electron-transporting layers, respectively. TPBI was also used as a host material in Device III. For comparison purpose, Device I and III were designed as reference devices. We were quite surprised at the very similar EL spectra of Device I and II (**Figure 5-6(a)**) and the performance of two OLEDs were quite similar. Both OLEDs exhibit deep blue EL with λ_{max} at 454 nm and 450 nm, respectively. They corresponds to CIE coordinates, x = 0.14 and 0.14, y = 0.10 and 0.09, respectively (**Table 5-2**). Device I and II showed maximum electroluminescence of 11500 and 10900 cd/m^2 as well as 670 and 685 cd/m^2 at current density of 20 mA/cm^2, respectively. External quantum efficiency of two devices is 3.8 and 4.0%, respectively (**Table 5-2**). Having exactly same CIE coordinate x = 0.14 and 0.09, Device III containing no **MADN** but **oFPhFBT**, showed significantly worse device performance. With the specific device configuration, CBP layer preventing the EL from NPB and the short wavelength emission (λ_{max} < 400 nm) of the host TPBI, Device III displayed indisputable EL from **oFPhFBT** and it is very similar to that of **MADN**. Considering there is very limited spectral overlapping between the sbsorption spectra of **oFPhFBT** and photoluminescence spectra of **MADN** (**Figure 5-7(b)**), we have a doubt about the orgin of EL of Device II. Furthermore, based on the relative position of HOMO/LUMO energy levels (**Figure 5-7(a)**), **oFPhFBT** is not particularly better in charge-trapping than **MADN**. It is highly possible that dopant **oFPhFBT** Device II outputs EL not from **oFPhFBT** dopant but MADN host. Since Device II had somewhat better efficiency performance than Device I, **oFPhFBT** dopant does not play a role of brighter blue emitter but an efficient charge carrier that promote the EL efficiency.

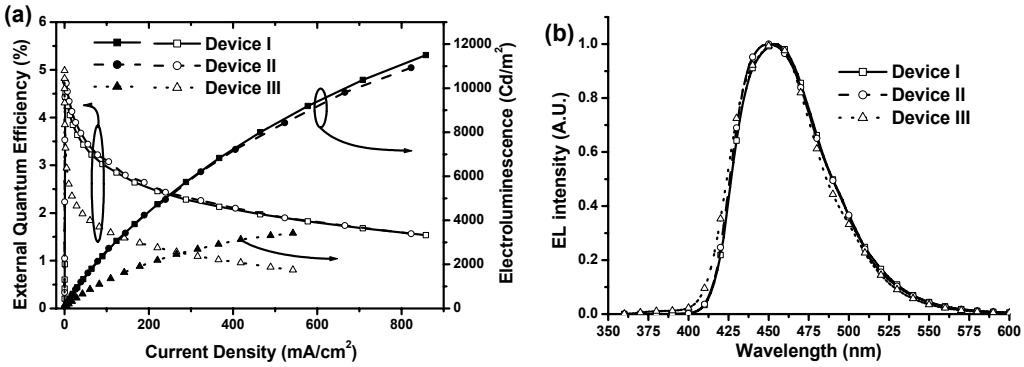

Figure 5-6. (a) Efficiency-current density- electroluminescence (η_{EXT}-*I*-*L*) characteristics of devices.; (b) The EL spectra of devices.

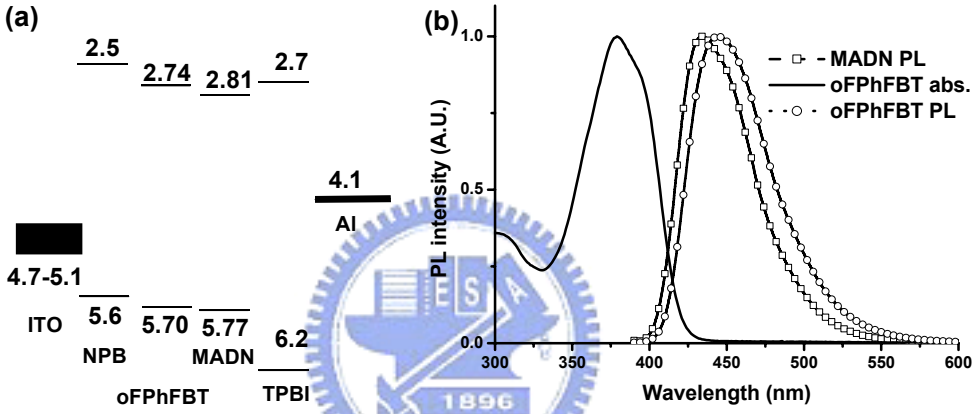

Figure 5-7. (a) The diagram of energy levels.; (b) the overlap of the absorption and PL spectra of **oFPhFBT** and the PL spectra of **MAND** in chlorobenzene.

5-4-3-2 Devices test of PhFBT

In order to investigate the light-emitting properties of doped **MADN** OLEDs, **PhFBT** was then chosen as the dopant material because of its high fluorescent quantum yield (74%) and its better spectral overlapping between the absorption of **PhFBT** and the emission of **MADN** (**Figure 5-8**), which is expected to have more efficient Förest energy transfer from **MADN** to **PhFBT**.

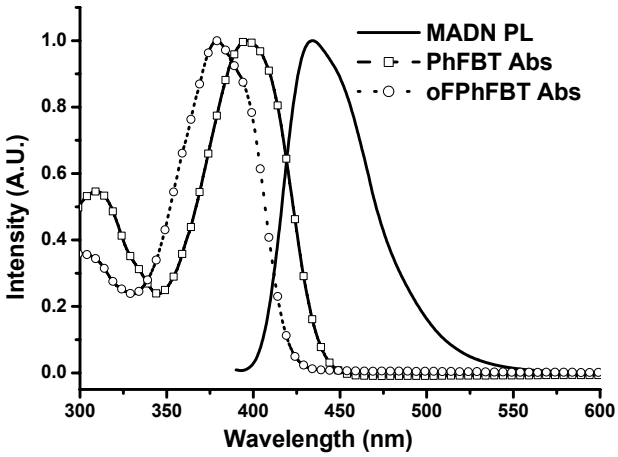

Figure 5-8. The overlap of the absorption spectra of **PhFBT** and **oFPhFBT** and the PL spectra of **MAND** in chlorobenzene.

Blue OLEDs based on **PhFBT** were fabricated as ITO/NPB (50 nm)/**MADN**: **PhFBT** (x%, 40nm)/TPBI (10 nm)/LiF (1 nm)/Al (150 nm), where doping concentration x is 0.5, 1, 3, 10, 20, 50, and 100, respectively. In these devices, TPBI was used not only a electron-transport layer but also a hole-blocking layer, in order to improve the charge recombination of hole and electron in the light-emitting layer. For the variation of electron-transporting layer, a reference OLED of ITO/NPB (50 nm)/**MADN** (40nm)/Alq_3 (10 nm)/LiF (1 nm)/Al (150 nm) was fabricated for testing. The reference **MADN** OLED shows poor external quantum efficiency of 1.74% at the current density of 20 mA/cm^2 with blue EL corresponding to CIE coordinate x = 0.5, y = 0.11. A puny shoulder (500 nm) was observed in the EL emission spectra which attributed to the contribution of electron transport layer Alq_3 emission (**Figure 5-9**). Therefore, this series of devices need an appropriate hole-blocking layer such as TPBI to prevent the emission from electron transporting layer.

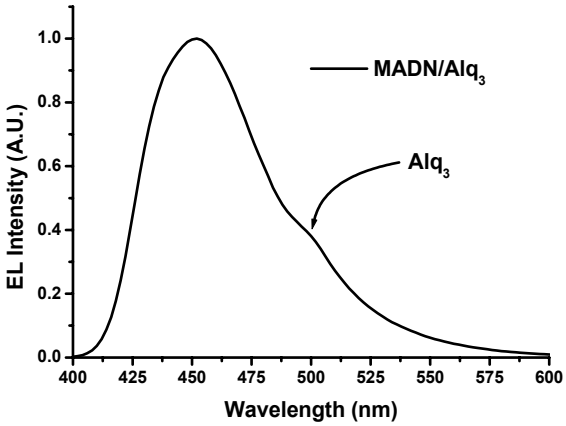

Figure 5-9. The EL spectrum of device ITO/NPB (50 nm)/**MADN** (40nm)/Alq_3 (10 nm)/LiF (1 nm)/Al (150 nm).

Table 5-3. Characteristics of OLEDs containing **PhFBT**.

dopant concentration[a]	Max. Luminance (cd/m^2)	Luminance, Efficiency, Voltage at 20 mA/cm^2 (cd/m^2,%, V)	λ_{max}^{el} (nm)	CIE 1931 Chromaticity (*x*, *y*)
0% (MADN)	11900	560, 3.7, 7.1	450	0.14, 0.08
0.5%	11800	680, 3.8, 6.6	450	0.14, 0.10
1%	12400	680, 3.9, 6.4	450	0.14, 0.10
3%	20500	810, 4.3, 5.6	452	0.14, 0.11
10%	28300	990, 4.7, 5.3	454	0.14, 0.13
20%	32300	1020, 4.1, 5.0	458	0.14, 0.15
50%	24000	690, 2.6, 4.5	460	0.13, 0.17
100% (PhFBT)	18300	400, 1.2, 4.2	466	0.14, 0.20

[a] ITO/NPB (50 nm)/ **MADN**:**PhFBT** (x%, 40nm)/TPBI (10 nm)/LiF (1 nm)/Al (150 nm)

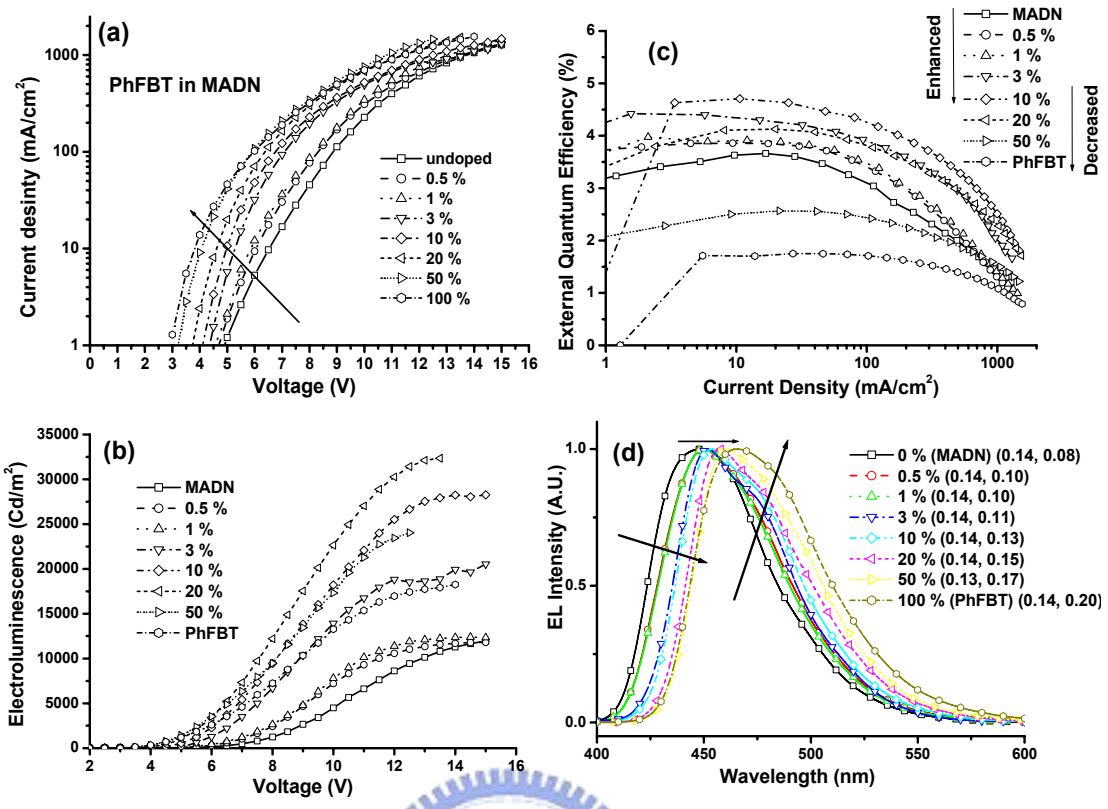

Figure 5-10. Electroluminescence (EL) characteristics of PhFBT based devices: (a) Current density-Voltage (*I-V*) characteristics; (b) Electroluminescence-Voltage (*L-V*) characteristics; (c) Efficiency-current density (η_{EXT}-*I*) characteristics; (d) The EL spectra of devices.

Data of **PhFBT** are summarized in **Table 5-3**. From **Figure 5-10(a)**, it is evident that the current density of these devices increases when the dopant concentration decreases. The EL emission bands are shifted gradually from 450 to 466 nm with the increase of dopant concentration from 0 to 100% (**Figure 5-8(d)**). This phenomenon was attributed to dual charge-transporting feature, namely arylamine and benzothiazloe of **PhFBT**. The best EL performance observed for device containing 10% of **PhFBT** dopant. It has EL external quantum efficiency of 4.7% at the current density of 20 mA/cm^2 (or at 5.3 V), maximum brightness of 28300 cd/m^2 or 990 cd/m^2 at the current density of 20 mA/cm^2, and EL λ_{max} of 454 nm corresponding to CIE coordinates x = 0.14, y = 0.13. From **Figure 5-8(c)**, it seems that the device performance (external quantum efficiency) is enhanced as the dopant concentration increase from 0 to 10% and the device performance decreases as the dopant concentration further increase to 100% because of the concentration quenching. This is

quite unusual that the optimal dopant concentration of PhFBT OLEDs is 10~20%, which is much higher than conventional figure ~3%.[10, 13]

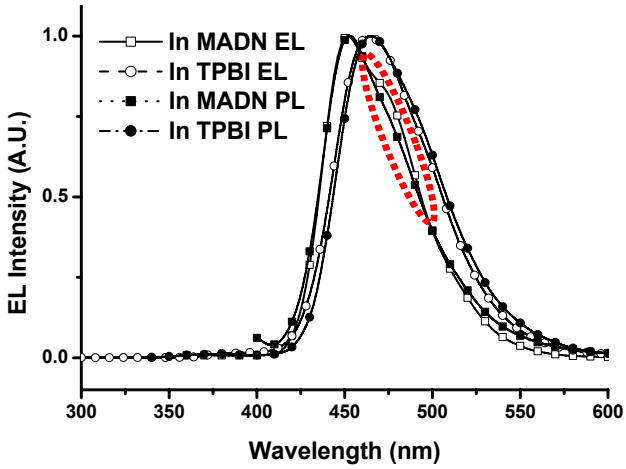

Figure 5-11. The overlap of the film PL and device EL spectra of 3% **PhFBT** in **MADN** or TPBI.

We believe that the EL contribution of these OLEDs is not only **PhFBT** dopant but also **MADN** host. In order to verify our conjecture, another reference device was fabricated as ITO/NPB (30 nm)/CBP (20 nm)/**TPBI**:**PhFBT** (3%, 40nm)/TPBI (10 nm)/LiF (1 nm)/Al (150 nm). From **Figure 5-11**, there is no **TPBI** emission peak at the wavelength of 380 nm that is known for EL λ_{max} of **TPBI**. A complete Förest energy transfer from **TPBI** to **PhFBT** or dominated charge-trapping of **PhFBT** instead of MADN is the fact for thus reference OLED. Similar conclusion can be made from the PL spectra of these system (**Figure 5-11**). A genuine **PhFBT** EL was observed herein at the λ_{max} of 468 nm which is quite different from the EL spectra (λ_{max} of 454 nm) of the same **PhFBT** concentration in **MADN**. It appears that the shoulder in the EL spectra of 3% **PhFBT** doped in **MADN** can be attributed to **PhFBT** emission (**Figure 5-11**). The contribution of the emission from **PhFBT** and **MADN** is clearly differentiable in the PL spectra of **MADN** their film samples doped with **PhFBT** (**Figure 5-12**). Therefore, we can now conclude that both dopant and host contribute EL (in **PhFBT** dopaed **MADN** OLED).

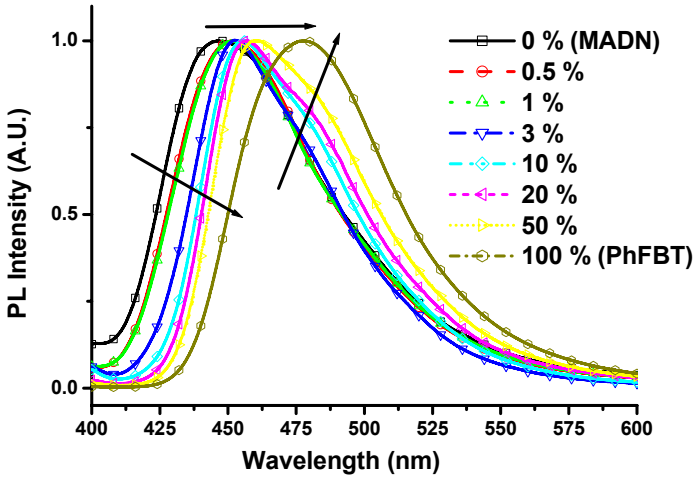

Figure 5-12. The film PL spectra of x% **PhFBT** in **MADN** at room temperature.

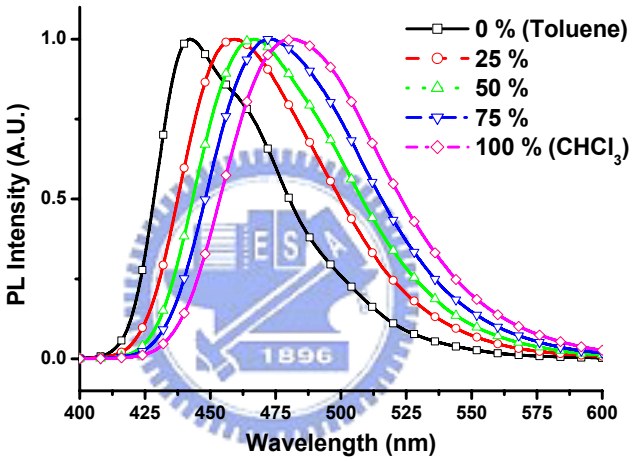

Figure 5-13. The PL spectra of **PhFBT** with increasing solvent polarity (in the cosolvent of toluene and $CHCl_3$).

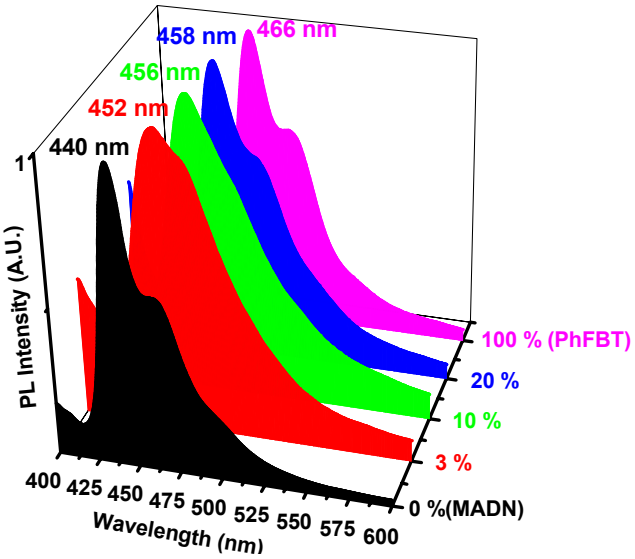

Figure 5-14. The film PL spectra of x% **PhFBT** in **MADN** at ~100 K

PL of **MADN** thin films doped with **PhFBT** having varied concentration of 0, 3, 10, 20, and 100% (neat **PhFBT** thin film) was investigated in probing the Frörster energy transfer from **MADN** host to **PhFBT** dopant. Room temperature PL spectra are shown in **Figure 5-12** and they display a red-shifting of emission bands along with the increase of dopant concentration, which is very similar to that of EL spectra shown in **Figure 5-10(d)**. Such red-shifting emission spectra can be attributed to the solvatochromism of dopant of which polarity exerting on the thin film. Solvatochromic shift of solution emission spectra of **PhFBT** is clearly shown in **Figure 5-13**. To clarify the composition of the emission bands in **Figure 5-10(d)**, we compare the PL spectrum of **MADN** thin film containing 3% **PhFBT** with that of **TPBI** thin film containing 3% **PhFBT** (**Figure 5-11**). We can identify that two PL spectra are quite different in terms of emission λ_{max}: the former is around 450 nm and the latter is around 470 nm. We note that the emission band of **PhFBT** doped **MADN** has a small shoulder (emission side band) discernible between 460~480 nm, which is very close to the emission λ_{max} of the **TPBI** thin film containing 3% **PhFBT**. In addition, for **PhFBT** doped **TPBI** thin film, there is essentially no detectable emission band from TPBI around 380 nm. Within this context, we can conclude that Förster energy transfer is quite efficient in the **PhFBT** doped **TPBI** thin film, whereas it is rather inefficient in the **PhFBT** doped **MADN** thin film.

Whereas room temperature PL spectra shown in **Figure 5-12** are hard to offer information in detail, low temperature (~100 K) PL spectra shown in **Figure 5-14** provide a much more insight about the composition of the emission bands of **PhFBT** doped **MADN** thin film. Vibronic emission bands (0-1 and 0-2) of either neat **MADN** (0% **PhFBT** dopant) or neat **PhFBT** (100% **PhFBT** dopant) can be clearly identified in **Figure 5-13**. Coincidentally, 0-0 emission λ_{max} of **PhFBT** (~470 nm) is almost same as the first vibronic emission (0-1) of **MADN**. Progressive red-shifting of the PL spectra observed for **MADN** thin films with increasing **PhFBT** dopant concentration is due the collective emission from

both **PhFBT** dopant and **MADN** host.

5-5 Conclusion

In summary, we have successfully designed and prepared a series of benzothiazole-carrying diarlyamino fluorene or spirobifluorene fluorophores. It is easy to blue-shift fluorescence to deep blue region by the introduction of methyl, chloro, or fluoro substituent to the ortho-position of diphenylamino donor. These fluorene or spirobifluorene fluorophores show high fluorescent quantum yields in a range of 54-74%, which are reasonably good for high efficiency blue OLEDs. High performance blue OLEDs containing **PhFBT**-doped **MADN** has been obtained with high dopant concentration of 10~20%. Emission λ_{max} at 450 nm corresponding to CIE coordinate, x = 0.14, y = 0.13 is one of the best authentic blue EL ever been achieved. Blue EL emission is attributed to both **PhFBT** dopant and **MADN** host due to the incomplete Förest energy transfer or similar charge-trapping ability of the two materials. The dual charge-transport characteristic of these bipolar fluorene or spirobifluorene blue dopant is also a key factor in enhancing performance of **MADN**-based OLEDs.

5-6 Reference

[1] (a) Forrest, S. R. *Nature* **2004**, *428*, 911.; (b) Kraft, A.; Grimsdale, A. C.; Holmes, A. B. *Angew. Chem. Int. Ed.* **1998**, *37*, 402.; (c) Mischke, U.; Bäuerle, P. *J. Mater. Chem.* **2000**, *10*, 1471.; (d) Kim, D. Y.; Cho, H. N.; Kim, C. Y. *Prog. Polym. Sci.* **2000**, *25*, 1089.; (e) Kulkarni, A. P.; Tonzola, C. J.; Babel, A.; Jenekne, S. A. *Chem. Mater.* **2004**, *16*, 4556.; (f) Gong, X.; Iyer, P. K.; Moses, D.; Bazan, G. C. Heeger, A. J.; Xiao, S. S. *Adv. Funct. Mater.* **2003**, *13*, 325.; (g) Hung, L. S.; Chen, C. H. *Mater. Sci. Eng.* **2002**, *R39*, 143.

[2] (a) Wen, S.-W.; Lee, M.-T.; Chen, C. H. *IEEE J. Display Tech.* **2005**, *1*, 90.

[3] (a) Hosokawa, C.; Higashi, H.; Nakamura, H.; Kusumoto, T. *Appl. Phys. Lett.* **1995**, *67*, 3853.; (b) Shaheen, S. E.; Jabbour, G. E.; Morell, M. M.; Kawabe, Y.; Kippelen, B.; Peyghambarian, N.; Nabor, M.-F.; Schlaf, R.; Mash, E. A.; Armstrong, N. R. *J. Appl. Phys.* **1998**, *84*, 2324.; (c) Lee , M.-T.; Chen, H.-H.; Liao, C.-H.; Tsai, C.-H.; Chen, C. H. *Appl. Phys. Lett.* **2004**, *85*, 3301.; (d) Kishigami, Y.; Tsubaki, K.; Kondo, Y.; Kido, J. *Synth. Met.* **2005**, *153*, 241.

[4] (a) Shi, J. Tang, C. W. *Appl. Phys. Lett.* **2002**, *80*, 3201. (b) Gebeyehu, D.; Walzer, K.; He, G.; Pfeiffer, M.; Leo, K.; Brandt, J.; Gerhard, A.; Stößel,P.; Vestweber, H. *Synth. Met.* **2005**, *148*, 205.; (c) Li, Y.; Fung, M. K.; Xie, Z.; Lee, S.-T.; Hung, L.-S.; Shi, J. *Adv. Mater.* **2002**, *14*, 1317.; (d) Kan, Y.; Wang, L.; Duan, L.; Hu, Y.; Wu, G.; Qiu, Y. *Appl. Phys. Lett.* **2004**, *84*, 1513.; (e) Kim, Y.-H.; Jeong, H.-C.; Kim, S.-H.; Yang, K.; Kwon, S.-K. *Adv. Funct. Mater.* **2005**, *15*, 1799.

[5] (a) Salbeck, J.; Yu, N.; Bauer, J.; Weissortel, F.; Bestgen, H. *Synth. Met.* **1997**, *91*, 209.; (b) Kim, Y.-H.; Shin, D.-C.; Kim, S.-H.; Ko, C.-H.; Yu, H.-S.; Chae, Y.-S.; Kwon, S.-K. *Adv. Mater.* **2001**, *13*, 1690.; (c) Tao, S.; Peng, Z.; Zhang, X.; Wang, P.; Lee, C.-S.; Lee, S.-T. *Adv. Funct. Mater.* **2005**, ***15***, 1716.; (d) Shen, W.-J.; Dodda, R.; Wu, C.-C.; Wu, F.-I.; Liu, T.-H.; Chen,H.-H.; Chen, C. H.; Shu, C.-F. *Chem. Mater.* **2004**, *16*, 930.; (e) Wu, C. C.; Lin, Y. T.; Chiang, H. H.; Cho, T.-Y.; Chen, C.-W.; Wong, K.-T.; Liao, Y.-L.; Lee, G.-H.; Peng, S.-M. *Appl. Phys. Lett.* **2002**, *81*, 577.; (f) Chen, C.-H.; Wu, F.-I.; Shu, C.-F.; Chien, C.-H.; Tao, Y.-T. *J. Mater. Chem.* **2004**, *14*, 1585.

[6] (a) Wu, C.-C.; Lin, Y.-T.; Wong, K.-T.; Chen, R.-T.; Chien, Y.-Y. *Adv. Mater.* **2004**, *16*, 61.; (b) Li, T.; Yamamoto, T.; Lan, H.-L.; Kido, J. *Polym. Adv. Technol.* **2004**, ***15***, 266.; (c) Markham, J. P. J.; Namdas, E. B.; Anthopoulos, T. D.; Samuel, I. D. W.; Richards, G. J.; Burn, P. L. *Appl. Phys. Lett.* **2004**, *85*, 1463.; (d) Wong, K.-T.; Chen, R.-T.; Fang, F.-C.; Wu, C.-C.; Lin, Y.-T. *Org. Lett.* **2005**, *7*, 1979.

[7] Tonzola, C. J.; Kulkarni, A. P.; Gifford, A. P.; Kaminsky, W.; Jenekhe, S. A. *Adv. Mater.* **2007**, *17*, 864.

[8] Chan, L.-H.; Lee, R.-H.; Hsieh, C.-F.; Yeh, H.-C.; Chen, C.-T. *J. Am. Chem. Soc.* **2002**, *124*, 6469.

[9] (a) Tamao, K.; Uchida, M.; Izumizawa, T.; Furukawa, K.; Yamaguchi, S. *J. Am. Chem. Soc.* **1996**, *118*, 11974.; (b) Tabatake, S.; Naka, S.; Okada, H.; Onnagawa, H.; Uchida, M.; Nakano, T.; Furukawa, K. *Jpn. J. Appl. Phys.* **2002**, *41*, 6582.; (c) Uchida, M.; Izumizawa, T.; Nakano, T.; Yamaguchi, S.; Tamao, K.; Furukawa, K. *Chem. Mater.* **2001**, *13*, 2680.; (d) Palilis, L. C.; Ma¨kinen, A. J.; Uchida, M.; Kafafi, Z. H. *Appl. Phys. Lett.* **2003**, *82*, 2209.; (e) Murata, H.; Kafafi, Z. H.; Uchida, M. *Appl. Phys. Lett.* **2002**, *80*, 189.

[10] (a) Ho, M.-H.; Wu, Y.-S.; Wen, S.-W.; Lee, M.-T.; Chen, T.-M.; Chen, C. H.; Kwok, K.-C.; So, S.-K.; Yeung, K.-T.; Chen, Y.-K.; Gao, Z.-Q. *Appl. Phys. Lett.* **2006**, *89*, 252903.; (b) Liao, C.-H.; Lee, M.-T.; Tsai, C.-H.; Chen, C. H. *Appl. Phys. Lett.* **2005**, *86*, 203507.; (c) Lee, M.-T.; Liao, C.-H.; Tsai, C.-H.; Chen, C. H. *Adv. Mater.* **2005**, *17*, 2493.; (d) Lin, M.-F.; Wang, L.; Wong, W.-K.; Cheah, K.-W.; Tam, H.-L.; Lee , M.-T.; Chen, C. H. *Appl. Phys. Lett.* **2006**, *89*, 121913.

[11] Hosokawa, C.; Hihashi, H.; Nakamura, H.; Kusumoto, T. *Appl. Phys. Lett.* **1995**, *67*, 3853.

[12] Li, H.-C.; Lin, Y.-P.; chou, P.-T.; Cheng, Y.-M.; Liu, R.-S. *Adv. Funct. Mater.* **2007**, *17*, 520.

[13] Okumoto, K.; Kanno, H.; Hamasa, Y.; Takahashi, H.; Shibata, K. *Appl. Phys. Lett.* **2006**, *89*, 013502.

Appendix
^{1}H and ^{13}C NMR spectra